About the frontier between filling and reinforcement by fine flax particles in plant fibre composites

Alain Bourmaud, Claire Mayer-Laigle, Christophe Baley, Johnny Beaugrand

About the frontier between filling and reinforcement by fine flax particles in plant fibre composites

[1]Alain Bourmaud, [2]Claire Mayer-Laigle, [1]Christophe Baley, [3,4]Johnny Beaugrand

(1) Univ. Bretagne Sud, UMR CNRS 6027, IRDL, F-56100 Lorient, France

(2) IATE, Univ Montpellier, CIRAD, INRA, Montpellier SupAgro, Montpellier, France

(3) Biopolymères Interactions Assemblages (BIA), INRA, rue de la Géraudière, F-44316 Nantes, France

(4) Fractionnement des Agro Ressources et Environnement (FARE), INRA, Université de Reims Champagne-Ardenne, 2 esplanade Roland Garros, F-51100 Reims, France

Corresponding author: Alain Bourmaud, alain.bourmaud@univ-ubs.fr

Abstract

Whatever in pulp or biocomposite sectors, the elements called fines coming from plant fibres have generally a length lesser than 200µm. Their mechanical impact has long been debated in short plant fibre thermoplastic composites. Are they solely a filling agent or on the contrary, have they a potential of reinforcement in such composites depending on their numbers, their length and aspect ratio? This work proposes an original experimental approach to explore the mechanical role of fine flax particles. Based on controlled milling of an initially homogeneous flax fibre batch that provides a population of fines (99% under 200µm, average Lw of 147µm), we devised a set of composites made of an increasing content of flax fines (0, 3.1, 5.6, 12.3, 20.4, 34.6 and 40.2%-vol) mixed with poly(propylene) (PP) and maleic anhydrid grafted PP (PP-PPgMA). Reference composites reinforced with chalk and also with cut flax fibre (Lw of 2000 µm) were also manufactured and studied. Results demonstrate that, despite a low aspect ratio (5±0.2 for 20.4%-vol), fines can act more than as just a simple filler, a slight modulus reinforcement is depicted but only beyond a high threshold of about 20%-vol (+29% compared to raw PP for 20.4%-vol). In addition to PP, we then investigated the mechanical influence of the flax fines in two representative matrix thermoplastic families Poly(amide)-11 (PA11) and poly(butylene-succinate) (PBS). We highlighted an increase of the Young's modulus of PA11 and PBS fines composites (+41%

and +115, respectively for 20.4%-vol), whereas strengths were lower compared to the respective neat polymers, exhibiting the possible negative role of fines on composite mechanical properties.

Key-words: Flax fibre; Fines elements; Thermoplastic polymer; Extrusion; Rheology; Mechanical properties; Fibre length

1. Introduction

The transformation of composites reinforced with plant fibres is developing and is now reaching a level of maturity in numerous industries, to manufacture products such as automotive non-woven parts (Renouard et al., 2017), sporting goods (Mohanty et al., 2018) as well as for original applications due to their specific hygroscopic behaviour (Abida et al., 2019; Duigou and Castro, 2017). However, the knowledge of these materials still needs to be progressed; not all reinforcement mechanisms or the specificities of these fibres are yet mastered. This is particularly true in the case of extruded and injected blends where the behaviour of the fibres, very different from that of the synthetic reinforcements, has a direct impact on the microstructure (Bourmaud et al., 2013) and consequently on the performance of the composites.

Plant fibres have a very specific structure (Goudenhooft et al., 2019, 2018). It is possible to assimilate them to a tubular composite structure consisting of a stack of plies, each having a different microstructure (Bourmaud et al., 2018). In the case of flax, this stack consists of a primary wall and a secondary wall consisting of 2 main layers S1 and S2. The major layer S2 represents about 80% of the fibre section and consists of cellulose fibrils inserted into a matrix of non-cellulosic polymers. These fibrils are oriented with a micro fibrillar angle (MFA) of about 10° with the axis of the fibre which gives it remarkable mechanical performances. In some cases, an S3 layer is present; its origin depends on the maturity of the wall; it is a portion, often minimal, of the S2 layer that has not reached full maturity. Thus, the breaking and damage mechanisms of a plant fibre (Beaugrand et al., 2017; Hughes, 2012) are very different from those of a synthetic fibre for which the breaks occur mainly in areas of defects created during the extrusion of the fibres. Flax fibres also have surface defects, called kink bands (Baley, 2004), which are preferred breaking zones. This was demonstrated through optical rheology by Le Duc et al. (Le Duc et al., 2011) ; the link between the distance between defects, such as kink bands, and final lengths of flax fibres after injection was confirmed by Gourier et al. (Gourier et al., 2017) on PA11-flax composites.

During an extrusion or injection process of a molten polymer, the reinforcing fibres are subjected to numerous thermomechanical stresses; in particular, during the compounding

phase in a twin screw extruder, fibres are submitted to mixing, shearing, conveying or a combination of these actions (Albrecht et al., 2018; Gallos et al., 2017). The intensity of these damages and final fibre length may vary according to the screw profile can consequently causes a reduction of the fibre length. Berzin et al. (Berzin et al., 2014) have shown that the decrease in the length of hemp fibre occurred principally in the mixing zones. These mixing zones consist of shearing elements causing the fibre to break. The process conditions used during compounding also have a crucial influence. During the injection step, most aggressive steps are the plasticizing and injection phases where the most shearing occurs, which strongly modifies the morphology of the fibres. The greatest reduction in fibre length occurs at the beginning of plasticization, under the effect of high shear stresses due to solid//molten interactions (Gupta et al., 1989). Although the greatest reduction in fibre length is due to the compounding step, the injection step again significantly impacts the lengths (Ausias et al., 2013). Thus, during a processing cycle, the plant fibres will show significant decreases in length but also in diameter because they are originally assembled into cohesive bundles in the plants (Goudenhooft et al., 2017). As the number of cycles increases, the lengths and diameters decrease, which allows the plant fibre reinforcements to have a relatively stable aspect ratio (L/D) over the cycles (Bourmaud and Baley, 2007), unlike glass fibres.

Whilst in most studies on the subject, the evolution of fibre geometry is highlighted, the finest particles, so called fines, are often neglected, arguably due to technical limitations because of the difficulty in measuring them. They were first defined in the pulping sector as particles or fragments being smaller than 150 microns in size (Ferreira et al., 1999); other limits were defined between 150 and 300 microns in length for biocomposite materials (Beaugrand and Berzin, 2013; Teuber et al., 2016). Fine particles resulted from the breakage of the elementary fibres or bundles during processing; they are generated at the same time by the ruptures of the fibres in their length (Thygesen et al., 2014) but also by the destructuring of the plant cell. Le Moigne et al. (Le Moigne et al., 2011) demonstrated that manual optical measurement methods could not identify them and that only automated optical analysis systems could reliably quantify these fines fibre elements. Recently the generation of fines attracted consideration in wood polymer composites (WPC), where Teuber et al. (Teuber et al., 2016) monitored a high quantity of fines according to twin screw processing parameters. For plant fibres, fewer studies on fines and their impact are available. Bourmaud et al. (Bourmaud et al., 2016a) studied the evolution of their content in case of PP-flax blends recycling; it was shown that fines were present in batches of cut fibres even before their introduction into the polymer at fractions of about 30% by number; after a extrusion and injection cycles, their ratio increases tremendously up to 90% by number. Their presence is therefore not anecdotal and they can potentially constitute an important bottle neck for the recycling of biocomposites. Furthermore, when part design and numerical modelling are

carried out, a fibre's aspect ratio is considered to estimate composite properties but the presence of fines particles is ignored, resulting in an overestimation of this aspect ratio, which is one of the main relevant indicators that define the fibre's potential of reinforcement. From the compounding community, it is admitted that the fines, arbitrarily considered as particles of lengths longer than 200 µm (Beaugrand and Berzin, 2013; Le Moigne et al., 2011), have a role more as a filler rather than a reinforcement. It is generally stated that both reinforcements and fillers induce an increase of the composite stiffness whereas a reinforcement increases also the material strength.

The objective of this work is to study the impact of flax fines particles on mechanical properties of a range of biocomposites. Firstly, batches of flax fines particles were artificially created by a suitable grinding technology and then characterized. Then, the mechanical behaviour of PP-PPgMA matrix composites made with an increasing volume fraction of flax fines (from 0 to 40.2%-vol) was studied and compared with composites reinforced with 2 mm cut flax fibres. The PP-g-MA fines composites were benchmarked with chalk, and also to a ternary mix of fibre + fines. In addition, 20.4%-vol composites were manufactured with PA11 and PBS matrices to deeper investigate the fines mechanical impact according to the various rheological grades of polymers. For each of these batches the tensile and impact mechanical performances were investigated.

2. **Experimental section:**

2.1 Materials

The flax fibre (*Linum usitatissimum L.*) used in this study is from the Alizée variety (harvested in 2015) and was cultivated in Normandy (France). Flax seeds were sown in March. As growth is temperature and humidity dependent, the plants were pulled out of the ground at the end of June, when the conventional cumulated degree of temperature was raised. The plants were then laid on the soil to enable dew-retting. After the harvest, the plants were stored, scutched and the fibres carded and cut into 2 mm lengths. The tensile Young's modulus, strength and elongation at break of the elementary fibres are shown in Table 1 (Bourmaud et al., 2015), respectively. The average diameter of the elementary fibres was measured to be 15.5 ± 2.7 µm, as determined by optical microscopy for 400 fibres after inclusion in epoxy resin and polishing of the section (Bourmaud et al., 2015). In order to produce flax fines, the flax fibres were ground in a vibratory batch ball mill DM1 (SWECO, USA). Basically, the milling device consists of a grinding chamber of 36 litres in abrasion-resistant elastomer which is filled with milling media and product to grind. The chamber is set in motion by a vibrating mechanism composed of high-tensile steel springs. Here, 1 kg of flax

fibres was preliminary dried in an oven at 60 °C for 24 hours, and was put into the milling chamber filled with 25 kg of ceramic cylinders (diameter and length: 13.5 mm) and 25 kg of ceramic balls (diameter 13.5 mm). This combination, by reducing the voids between the milling media maximizes the friction and optimizes the grinding. The milling time (23 hours) was determined based on preliminary tests so that the 90th percentile of the particle size distribution (d90) was below 200 microns. To be consistent with previous studies (Berzin et al., 2014; Le Moigne et al., 2011; Teuber et al., 2016) about the presence or aim of fines in plant fibres biocomposites, the length of 200 µm was considered to be the lower limit to speak about fibres; fines being below this limit. To produce enough flax fines, 2 batches of 1 kg were produced and they were homogenized in a Turbula® T10 B blender (WAB, Germany) for 10 min.

The chalk (CaCO3) used in this study is a commercial grade (Omyalite®) from OMYA (France). This component is generally added to decrease the cost of formulations or to improve their processability, stiffness or viscosity. Here, it plays a baseline function, giving a suitable reference for comparison with flax fines regarding their respective morphologies. The main objective of the introduction of chalk in the study is to compare mechanical reinforcement of chalk with fine's one.

Three different matrices have been used, PP-PPgMA as a reference and due to its broad use in biocomposite industry, the PPgMA has an proved effect on chemical bonding of the polymers and particles in the compound (Felix and Gatenholm, 1991; Graupner et al., 2014). In addition, PA11 and PBS were used; they have demonstrated a very interesting potential, when used with plant fibres, due to their easy process and their good affinity with plant cell walls (Bourmaud et al., 2016b, 2015). The first is a poly-(propylene) (PP) PPC10642 from Total Petrochemicals®. The melt flow index of this PP injection grade is 44 g/10 min at 230°C (under a load of 2.16 kg). In order to improve the compatibility between the fibres and the PP matrix, we used a maleic anhydride grafted PP (PPgMA), OREVAC 100, from Total Petrochemicals®, which is a PP with 4 wt% of PPgMA. The poly-(butylene-succinate) (PBS) used in this study is Bionolle 1020 MD supplied by Showa Denko (Tokyo, Japan) with a Melt Flow Index (MFI) of 20–34 g/10 min (at 140 °C and 2.16 kg) and a density of 1.26 g/cm3. poly-(amide 11) (PA11) under the trade name Rilsan PM 11 LMFO is supplied by ARKEMA in pellet form with a Melt Flow Index (MFI) of 25 g/10 min (at 210 °C and 2.16 kg) and a density of 1.02 g/cm3. The average degrees of crystallinity and melt temperature of the PA11 matrix are 21.9 ± 1.8% and 188.7 ± 0.9°C, respectively (Bourmaud et al., 2016b).

2.2 Morphological analysis of fines and fibres before compounding

The particle size distribution of the flax fines and chalk powder was determined by laser diffraction using a laser diffraction particle size analyser Hydro 2000S (Malvern Instruments Ltd., United Kingdom) with a liquid ethanol (ethyl alcohol: 96% v/v) carrier to avoid particle swelling. The determination of the size is based on the assumption that particles are spheres and results are expressed in volume. This analysis technique is not adapted for raw flax fibres since they presented an elongated shape. Thus, the size and shape of the raw flaw fibre were determined using a prototype (Berzin et al., 2014) MorFi automatic analyser (Techpap, Grenoble, France) fully described in (Di Giuseppe et al., 2016). To do so, a precise mass of approximately 0.1 g was diluted in distilled water, and the fibre's elements were tested in triplicate samples to determine their length mean values. The length is a characteristic fibre element size, one of the three relevant morphometric features identified earlier for a fibre element population morphology description (Legland and Beaugrand, 2013). Over 8,000 fibre elements were counted for each sample, and the results were expressed in mean values.

2.3 Scanning Electron Microscope analysis

Fibres, fines and chalk were metallized with gold before being observed through a JEOL JSM 6460LV (Jeol, Croissy Sur Seine, France) scanning electron microscope (SEM).

2.4 Thermogravimetric analysis

Experiments were performed using a SetaramTM 92 apparatus. The heating rate was 10°C /min under air atmosphere from 25°C to 900°C. Around 40 mg of each kind of fibre was used. Changes in weight versus temperature were recorded.

2.5 Compounding and processing

Both the flax fibres and fines were dried under vacuum at 60°C for 12hrs prior to the extrusion step. Composites were prepared using a laboratory-scale twin-screw co-rotating extruder ZSE 27 MAXX Torque (Leistritz, Germany) having a screw diameter of 28.3 mm, and length/diameter ratio of 36. The screw profile is detailed in Figure 1. The twin-screw profile included in addition conveyed elements to a venting zone for the evacuation of water steam and a kneading block after area 1, for the melting of the polymer matrix, and two extra mixing blocks after fibre introduction (area 2).

All mixtures, polymer, fines or chalk were introduced before the three shearing zones in position 2 (area 1, Fig 1). The flax fibres were introduced in area 2 (Fig 1) between the first and second shearing zones cutting-edge (in red in Figure 1). A fixed barrel temperature of

140 °C, 190 °C and 210 °C for PBS, PP-PPgMA and PA11 composites was set respectively. The total feed rate was 3 kg/h for all blends with a screw speed of 200 rpm. Table 2 collates the different elaborated compounds, according to the type of materials and weight fractions.

After the extrusion step, the formulations were immediately put into a cold-water container, and then pelletized into approx. 3 mm length granules. Injection moulding was carried out on a Battenfeld BA 800 machine. The mould temperature was maintained at 30 °C for all the compounds. The compounds were injected into a mould designed to produce ISO-527 normalized specimens. The screw temperature was fixed at 140 °C, 190 °C and 210 °C for PBS, PP-PPgMA and a PA11 matrix respectively.

2.6 Rheological experiments

To check the consistency with standard injected materials and record the recycling effect, the granulated composites were dried at 60°C for a period of 15h prior to testing. The tests were made on initial shredded plates and after each injection cycle (including the last injection using a compression moulding method). A capillary rheometer (Göttfert RG20, Göttfert, Buchen, Germany) was used to measure the shear viscosity of the melt. The barrel temperature was pre-set to 140 °C, 190 °C and 210 °C for PBS, PP-PPgMA and PA11 composites respectively. The samples were heated for 300s in the barrel and then extruded through 10, 20 and 30 mm lengths and 1 mm diameter dies. The experiments were performed at increasing shear rates of 10, 50, 100, 500, 1000, 2000, 5000 and 10000 s-1. The pressure needed to extrude the material through the 3 dies at each shear rate was recorded when constant (having less than 3% deviation) reading values were reached. After the experiments, the Bagley (Bagley, 1957) and Rabinowitsch (Rabinowitsch, 1929) correction was applied to correct the apparent shear rate and to calculate the true shear viscosity.

2.7 Morphological analysis of fines and fibres after compounding

For the measurement of the length of the fibre elements after processing each transformation cycle (extrusion coupled with injection) the fibre elements length distribution was quantified for the PP, PA11 and PBS-flax samples. At first, the PP and PBS matrices were extracted using a Soxhlet extraction methodology as described elsewhere (Berzin et al., 2014). The PA11 is extractable with trifluoroacetic acid (TFA, Sigma-Aldrich, Germany) and so PA11 composites were submitted to Soxhlet extraction. Several renewals of the TFA were necessary and the extraction duration took up to 3 days.

In this study, the average values L (geodesic length) and D in weight or ‘‘contraharmonic mean” are provided, and are also termed as average weight Lw, Dw. Thus the aspect ratio L/D is the (L/D)w .

2.8 Tensile characterisations

Static tensile tests were performed on a MTS Synergie RT/1000 tensile machine equipped by a 10 kN load cell and a 25 mm nominal length extensometer at a crosshead displacement speed of 1 mm/min. The values presented in this paper are average values of five reproducible tests, according to ISO-527-2. Prior to the tensile experiments, injected samples were conditioned for one week at 23°C and at a constant humidity of 48% RH. Average tensile modulus, strength and strain at break were calculated on at least 5 reproducible samples.

2.9 Impact test

Impact resistance of each material was characterized using a TINIUS OLSEN Model Impact 503 impact tester. Tests were carried out according to ISO 179-1 (non-notched Charpy impact) on 10 specimens measured and averaged. The following formula was used:

$$I_e = \frac{E_c}{h \cdot b} \cdot 10^3$$

With Ie the impact energy, Ec the absorbed energy (J), h and b the sample thickness and width (mm), respectively.

3. **Results and discussions**

3.1 Characterization of fines and fibres elements before compounding

3.1.1 SEM analysis

Figure 2 presents the observations obtained by SEM on the three types of reinforcements. The cut flax fibres (Figure 2.A) have on overall a satisfactory appearance with a homogeneous and regular surface. It is possible to distinguish kink-bands which are considered as zones of brittleness; it has been demonstrated that during a shaping process in a thermoplastic, the fibres break in a preferential way at their level (Le Duc et al., 2011). A correlation between the distance between defects and the final length of the flax fibres after

extrusion and injection has also been shown with a PA11 matrix (Gourier et al., 2017). Finally, on the surface of the fibres, we note the presence of residues of the middle lamellae or cortical walls which may result from moderate scutching or under retting of the plants; these pectic elements can be a drawback for the fibre-matrix interface in the case of severe sub retting (Le Duigou et al., 2012). As far as flax fines are concerned, a complete destructuring of the fibres can be noted; the initial geometry of the fibres is no longer visible, the efficiency of the selected grinding system is confirmed and interestingly, the morphologies of the generated fines are close to those that we observe in PP-PPgMA -flax composites after several cycles of recycling during previous works (Bourmaud et al., 2016a). The morphology of both chalk particles and clusters (Figure 2.C) follows with the objective of similarity to the ground flax fibres, confirming the relevance of the selection of this component as a reference. One can see that not one of the chalk and flax fines clusters are bigger than the other, but the regularity of the surface of the chalk seems higher than flax fines.

3.1.2 Morphological analysis

Figure 3 shows the length distribution of fibres and the particle size distribution for flax fines and chalk before incorporation into composites. Due to the contrasted aspect ratio of those particles, we chose to adapt our morphometric measurement in agreement, therefore the fibres (L greater than 200µm with a high L/D) were tested and measured using a Morfi automatic analyser. Whereas more reliable data were expected through laser diffraction analysis for flax fines and chalk (low L/D), one notes that the profile of flax fibre and fines differs greatly. Flax fibre exhibits a narrow and well centred distribution on the targeted length of 2 mm with an average length of 1811 µm (Table 3), highlighting the efficiency of the fibre cutting process; only a small population appears under 0.8 mm (Fig 3), probably representative of a fraction of small particles produced during this cutting step and confirming the presence of fines particles even in a batch of raw cut fibres (Bourmaud et al., 2016a). Conversely, the shape distribution of fines particles is less homogenous and wider, in good accordance with the SEM observation. Furthermore, 99.2% of the flax fines particles obtained after milling have a size below the targeted value of 200 □m; as evidenced on Figure 3, only a much reduced fraction of fines elements exhibit a size greater than this value.

Although its average dimensions are slightly smaller than those of fines particles and its distribution is narrower, we can consider that chalk powder particles represent a good basis for comparison in terms of reinforcement compared to fines. This filler is widely used in the field of thermoplastic composites and it will be interesting to compare the performances of composites reinforced with fines with those of chalk reinforced ones.

3.1.3 Thermal behaviour

Figure 4 shows the behaviour obtained through thermo gravimetric analysis for flax fibres and fines. For each type of reinforcement, 3 successive losses of mass can be distinguished, the first corresponds to the water loss of the plant walls, the second to the degradation of the components of the most heat-sensitive walls (pectins, hemicelluloses and amorphous cellulose) and the third to the loss of the most heat-resistant components such as condensed lignin or crystalline cellulose chains with high degrees of polymerization (Bourmaud et al., 2010). A lower thermal stability can be noted for fines; the inflection points of their mass loss curves occurring at a lower temperature of 35°C and 36°C for peaks 2 and 3, respectively, relative to the fibres. In addition, the quantity of degraded constituents is 6% higher than peak 2 for fines while it is 9% lower for peak 3; part of the constituents has therefore evolved during the process of milling flax fibre into fines, leading to an earlier thermal degradation of the latter. In addition, fines have a higher fraction of water, visible at the beginning of the curve, being 4.8% and 8.0% for fines and fibres, respectively.

These different findings can be related to the evolution of the structure of plant walls as well as to the data in the literature. It has been shown that severe ball milling results in a significant decrease in the crystallinity of plant walls (Khan et al., 2016; Nada et al., 1998) and an increase in their water absorption (Schell and Harwood, 1994; Tarafdar et al., 2001). As shown in Figure 2, ball milling results in a significant destructuring of the morphology of plant cell walls, making available both newly water bonding sites or porosity that favours water retention. In addition, the possible decrease in the crystallinity of cellulose after a milling phase is linked to a depolymerisation of a significant fraction of the most thermo stable cellulose; lignin can also be impacted by this depolymerisation. This evolution of the structure of the constituents generates a larger fraction of thermo labile polymers; the changes in thermal behaviour observed are in phase with these structural modifications.

3.2 Mechanical performances of fully flax fines or flax fibre PPgMA-composites

Figure 5 compares the mechanical performance of composites made with only fines or fibres. Tensile Young's moduli and strength at break are represented as a function of the volume fraction of reinforcements. A contrasted behaviour is observed between fines or fibres. For fibres, a linear increase in stiffness with fibre content is observed starting from roughly 6%-vol (10% wt) to nearly 37%-vol (50% wt%). When fines are used, an increase of the tangent Young’s modulus is observed but with a marked offset, in fact the increase starts only with 20.4%-vol and the slope is much less pronounced compared to the one of the fibre. This observation should be directly related to the aspect ratio of the particle components (Table 3) which was determined after PPgMA extraction of the solids phase on injected composites. The initial morphology and length of the introduced particles has a direct impact on the performance of the composites. The fines

demonstrate undoubtedly a measurable contribution in terms of material stiffness that one can consider as marginal compared to the fibre contribution. For instance, for a volume rate of approximately 37.4%, they produce an increase in modulus of +57% stiffness compared to PP-PPgMA alone, while the same increase is +254% if fibres are used; the fibres have better mechanical properties and their much higher aspect ratio enables them to align in the direction of flow and to reinforce composites much more effectively (Tanguy et al., 2018). This is roughly a ratio of 1/5 contribution for fines compared to fibres, and this only occurs with a large volume of fines (37.4% in our experimental procedure) when it has already increased stiffness with only 5.6%-vol fibres (Fig.5A). This result gives us a first indication of the influence of the presence of fines on the mechanical performance of associated composites.

Evolution of strength (Fig 5B) confirms this result; in the case of cut fibres, the tensile strength at break of the injected composites increases with the fibre volume content. Then, it decreases slightly beyond a specific content, corresponding to a critical fraction of reinforcements; above it, the significant volume of fibre bundles leads to the appearance of areas of weakness. The latter thus have preferential areas of rupture; this limit is about 32%-vol. When fines are added to the material, contrasted behaviour is experienced. The strength at break of the PP-PPgMA increases slightly as long as a minimal quantity of 3.1%-vol is added, but does not change thereafter regardless of the volume rate of fines added. The increase observed on the stiffness (Fig 5A) does not increase the strength values, which remain unchanged regardless of the volume rate of fines added. For a fines volume rate of 34%, the stress increase is only +24% compared to that of virgin PP-PPgMA, while it is +254% for a fibre volume rate of 32%, so an efficiency ratio of approximately 1/10, leads us to consider that the strength increase produced by the fines is negligible compared to fibre contribution.

Mechanically speaking, fines reinforced composites therefore have much lower properties in comparison to fibre composites. The lengths and aspect ratios of the introduced reinforcements play a major role and morphological differences of the raw reinforcements are reduced but are still present after an extrusion cycle and injection moulding (Table 3). In addition, the structure of the cell walls is considerably altered by the grinding process (Figure 2), as they cannot regain their original mechanical properties. Thermo gravimetric analyses have shown major changes in the properties and stability of flax fibres after severe grinding. The matrix and structural polymers of flax cell walls such as pectins, hemicelluloses and cellulose have been modified and arguably deconstructed, which in turn no longer allows them to play their mechanical or cohesive function, which is essential for fibres to display a high mechanical performance. Finally, the surface of the fibres has been modified, the destructuring of the walls makes some of their components accessible to the PP-PPgMA matrix; the coupling agent formulated to optimise the adhesion between poly(propylene) and the OH groups available on the fibre surface cannot fully fulfil its function, which is detrimental to the mechanical performance of the composites produced.

3.3 Ternary blends: evolution of composite performances according to the polymer matrix

3.3.1 Evolution of fibre length after processing

Table 3 shows the length of flax fines and fibres measured with the MorFi automatic analyzer after dissolution of the polymer matrix.

After the compounding and injection cycle with a poly(propylene) matrix, the morphology of the fines changes little; the aspect ratio and consequently the potential for particle reinforcement remain low. Flax fibres, despite a significant decrease in their length, retain an aspect ratio of 31 ± 4 due to the combined decrease in their diameters. We observe that this 18 ± 6 μm diameter is very close to that of the elementary flax fibres (15.85 ± 3.9 μm); the plant bundles initially present in the plant and still partially assembled after the scutching and cutting of the fibres, have undergone a complementary division during the transformation process, favourable to the reinforcement of the composites. The length of the fibres in the composite is close to 600 μm, which is consistent with the values usually found in the literature (Beaugrand and Berzin, 2013; Bourmaud et al., 2016a). Logically, for the PP-f-F-30 mixture, the morphological values of the reinforcements are positioned in an intermediate way between the fines and the fibres.

Depending on the nature of the matrix, the morphologies of the fibres differ after injection. PA11 has a high affinity for flax fibres (Le Duigou et al., 2016) and a much lower viscosity (Bourmaud et al., 2016b) than PP or PBS (Bourmaud et al., 2016a), which results in a significant break in fibre lengths of 434 ± 35 μm compared to 592 ± 183 and 497 ± 19 for PP and PBS respectively. This is probably due to a higher shear during the processing related to the fluidity of the polymer. Conversely, the fibre bundles appear less divided, which may appear contradictory. Its good adhesion to the fibres probably enables it to maintain a strong cohesion of the bundles during the process. PBS favours division, the average diameter of 14 ± 1 μm is similar to that of elemental flax fibres, whilst also reducing lengths significantly compared to the PP matrix. Of the three polymers, it is the most viscous, which seems to have a significant impact on the individualization of the reinforcements. Finally, we can assume that despite the meticulous extraction protocols, polymer extraction can sometimes be incomplete. In this way, the TFA used for PA11 extraction may have at least partially digested some flax particles, because this acid is often used for lignocellulose hydrolysis prior to biochemical investigation.

3.3.2 Rheological analysis

The influence of the presence of fines on the rheological properties of the biocomposites is studied by capillary rheology. Figure 6 shows the curves obtained on different PP-PPgMA matrix formulations. Generally speaking, one notes that the presence of particles significantly increases

411 the viscosity of the polymer, moderately for fines and much more so for flax fibres. Note that the
412 viscosity of the formulation containing only fines (30%wt) is very similar to that made with chalk
413 powder, which is a filling agent. Thus, the addition of fines in significant quantities only slightly
414 impede the viscosity of the composite, and these fines are not a drawback to the injection of thin
415 walls as can be the case with fibres. Regardless of the apparent viscosity curve considered, a
416 significant dependence on the shear rate can be observed (Steller, 2005); it is more pronounced
417 when fibres are added acting as a reinforcement. In addition, for low viscosities, the fibres are
418 entangled and poorly oriented in the direction of flow, which produces high viscosities compared
419 to the virgin polymer or reinforced by particles with smaller shape factors such as fines or chalk.
420 With an increasing shear rate, the viscosity of the composite decreases more significantly than
421 that of the virgin polymer, the reinforcements flow more easily. Flow properties can depend on
422 many factors such as the stiffness of the reinforcements, their adhesion to the matrix, the volume
423 ratio or their geometric characteristics. In our case, most of parameters are similar between the
424 mixtures and the main influential one, here it is morphology, and in particular the aspect ratio of
425 the particles. The work of Le Duc et al. (Le Duc et al., 2011) has shown that the viscosity of
426 composites reinforced by plant walls is influenced by the size of the reinforcements; when the
427 latter are less than 200 microns long, fibre-fibre interactions are reduced and the nature of the
428 flow is between a concentrated and semi-liquid mode; this is confirmed by our measurements, at
429 high shear rates. The viscosity of the composite reinforced by fines is very close to that of the
430 polymer, highlighting the low impact of the particles on its flow.

431

432 *3.3.3 Effect of the polymer matrix type on biocomposite mechanical*
433 *properties*

434 In addition to PP-PPgMA, in order to enlarge the range of polymer types, we have tested PBS
435 and PA11 polymers and assessed the influence of the polymer. Based on the PP results (Fig 5),
436 new tests with the upper rate above the threshold identified were performed; a loading rate of
437 30%-wt was chosen to be able to depict a putative specific polymer contribution. Figure 7 shows
438 the tensile mechanical properties of injection-moulded composites. With regard to Young's
439 modulus, a similar trend is observed according to the matrix used. Fibre materials are the most
440 efficient for reinforcement. As already shown in Figure 5, composites reinforced with fines
441 (30%wt) have a much lower stiffness, assumed to be due to the fines low aspect ratio, resulting in
442 a much lower reinforcement potential for fines than for fibres. Moreover, structural damages
443 during fines milling have probably induced a decrease of their mechanical performances. Fines-
444 fibre mixtures offer intermediate stiffness. However, it should be noted that a significant number
445 of fines are generated during the process (Bourmaud et al., 2016a) and that even fibre blends
446 contain a fraction of fines, especially after two processing cycles (extrusion-injection) as is the
447 case here. Given the shear rates involved, it is illusory to want to produce fractions composed

only of flax fibres by extrusion and injection. Note that fines have a higher reinforcement potential than chalk in terms of stiffness. Regardless of the matrix considered, the Young's modulus of fines composites is higher than that of mixtures containing chalk, this increase ranges from +17% for PP-PPgMA to +35% for PBS. Generally the stiffness of compounds containing PBS is greatly improved with the addition of fines or fibres. As far as fibres are concerned, a mass addition of 30% produces an increase in the modulus of the composite by +325% whereas it is only +163% with PA11 and +111% with PP-PPgMA; note that fibre elements extracted from PBS-F-30 composite exhibit the highest aspect ratio with a value of 38 (Table 3), especially by comparison with PA11, due to high viscosity of PA11 with the selected process conditions (Gourier et al., 2017).

The strength values (Figure 7) illustrate results depending on the nature of the matrix, a reinforcing effect is noted only for the PP-PPgMA matrix and only when fibres are used. The use of fines, chalk or fines-fibres never allows to increase the matrix strength whatever the considered polymer. Regarding the specific case of fines particles, probably due to the presence of reinforcement clusters generating areas of fragility, they do not improve the tensile strength when used alone or even mixed with flax fibres. Except for PP-F and PP-f-F compounds, the presence of reinforcement causes a systematic decrease in strength at max, which is less pronounced when fibres are introduced but remains significant; however, the stress levels of these matrices are high and if we take the case of PA11, the addition of 30% fines makes it possible to obtain a significantly higher strength than that obtained with PP-PPgMA -fibres. The level of tensile strength obtained, close to 40 MPa, is therefore quite satisfactory for a short fibre biocomposite. With the PA11 matrix, the strength reduction between the virgin matrix and compounds containing fines and fibres is -19% and -10%, respectively, while it is -39% and -12% with a PBS matrix. Despite the slight decrease observed when the reinforcements were introduced with PA11 and PBS, high levels of strength at break are maintained; with PP matrix the gap between polymer and composite strength is lower but the values reached do not enable to target semi-structural applications with fines or fines-fibres blends. As with the modulus, the aspect ratio (Table 2) of the reinforcements is also a major criterion for the mechanical performance of the materials.

Thus, mixtures containing fines have strength levels slightly lower than those containing chalk but their stiffness is significantly higher. The fines thus play a real role of mechanical reinforcement in such a tailored experiment where an uncommon rate of fines is use. Nevertheless, this latter remains very far from the potential of the fibres and their presence in a composite is finally quite strongly penalizing for its mechanical performances.

Finally, Figure 8 shows the impact energy of the various composites manufactured. The impact energies of the raw polymers or those reinforced with chalk were not illustrated, as these composites do not break during the tests. As with tensile strength at break results, the results are

not only strongly influenced by the nature of the particles but also by the matrices used. For the PP-PPgMA matrix, which has a low-quality interface with flax fibre, the nature of the reinforcement does not matter and the difference between fines and fibres is not significant. Conversely, for PA11 and PBS, the use of fibres rather than fines makes sense for impact resistance. This is particularly pronounced for PA11 compounds which have a very good interface with flax fibres. In this case, the presence of fines in the composite is very detrimental.

4. Conclusion

The objective of this work was to deeper understand the behaviour of flax fines particles within a thermoplastic polymer matrix and to estimate their reinforcement capacity. Even if the reinforcement capacity of the fines has been demonstrated in terms of stiffness, it remains modest compared to short flax fibres. The stiffness achieved with a 2 mm fibre volume fraction of 5.6% is only achieved with 37.4% of fines, i.e. a ratio of about 6.7. Their presence is therefore very detrimental in terms of reinforcement, especially since we have been able to show that in some composites they can reach rates of 90% in number. This low reinforcement capacity was confirmed with a panel of polymers, the mechanical performance of fines-strengthened polymers being much lower than those containing fibres, regardless of the matrix considered. This trend is also much more pronounced for tensile stress than for Young's modulus. This is confirmed when comparisons are made with chalk which has a morphology similar to that of fibres; chalk-reinforced polymers generally have higher tensile stresses than those reinforced with fines, but the stiffness of thin composites is better, probably due to their intrinsic performance and reinforcement structure.

Interestingly, fines particles induce a decrease in the viscosity of the mixtures which does not constitute a negative point but which will nevertheless impact the microstructure of the part and consequently its mechanical performance. Finally, with regard to impact performance, fines cause a decrease in absorbed energy, which is particularly visible for PA11 matrix composites. This can be explained by the high temperatures used during the processing of this polymer, due to the low thermal resistance of the fines compared to that of the fibres.

This work has shown that fines particles have a significant impact on the mechanical performance of biocomposites. They are generated by the processing cycles but also during the preparation of the fibres. Thus, their quantity must be reduced as much as possible so as not to damage the performance of composites. It is therefore important to limit process times and the number of transformation cycles, but also to adapt the extraction and cutting methods of the fibres to limit the quantity of fines within the parts as much as possible.

Acknowledgements

The authors would like to thank the French Environment and Energy Management Agency (ADEME), the French research cluster CNRS-INRA 'Symbiose' SYnthon et Matériaux BIOSourcés, for funding this work through the collaborative project RECYTAL and the French Research Ministry. They also acknowledge Victor Renvoizé and Cécile Sotto from the plant transformation platform of the JRU IATE for their experimental support. The authors would also like to thank also Miguel Pernes, Alain Lemaitre and Francois Gaudard from FARE for their contributions to the experiments.

Bibliography

Abida, M., Gehring, F., Mars, J., Vivet, A., Dammak, F., Haddar, M., 2019. Effect of hygroscopy on non-impregnated quasi-unidirectional flax reinforcement behaviour. Ind. Crops Prod. 128, 315–322. doi:https://doi.org/10.1016/j.indcrop.2018.11.008

Albrecht, K., Osswald, T., Baur, E., Meier, T., Wartzack, S., Müssig, J., 2018. Fibre Length Reduction in Natural Fibre-Reinforced Polymers during Compounding and Injection Moulding—Experiments Versus Numerical Prediction of Fibre Breakage. J. Compos. Sci. 2, 20–37. doi:10.3390/jcs2020020

Ausias, G., Bourmaud, A., Coroller, G., Baley, C., 2013. Study of the fibre morphology stability in polypropylene-flax composites. Polym. Degrad. Stab. 98, 1216–1224. doi:10.1016/j.polymdegradstab.2013.03.006

Bagley, E.B., 1957. End Corrections in the Capillary Flow of Polyethylene. J. Appl. Phys. 28, 624–627.

Baley, C., 2004. Influence of kink bands on the tensile strength of flax fibers. J. Mater. Sci. 39, 331–334.

Beaugrand, J., Berzin, F., 2013. Lignocellulosic fiber reinforced composites: Influence of compounding conditions on defibrization and mechanical properties. J. Appl. Polym. Sci. 128, 1227–1238. doi:10.1002/app.38468

Beaugrand, J., Guessasma, S., Maigret, J.-E., 2017. Damage mechanisms in defected natural fibers. Sci. Rep. 7, 14041. doi:10.1038/s41598-017-14514-6

Berzin, F., Vergnes, B., Beaugrand, J., 2014. Evolution of lignocellulosic fibre lengths along the screw profile during twin screw compounding with polycaprolactone. Compos. Part A Appl. Sci. Manuf. 59, 30–36. doi:10.1016/j.compositesa.2013.12.008

554 Bourmaud, A., Åkesson, D., Beaugrand, J., Le Duigou, A., Skrifvars, M., Baley, C., 2016a.
555 Recycling of L-Poly-(lactide)-Poly-(butylene-succinate)-flax biocomposite. Polym.
556 Degrad. Stab. 128, 77–88. doi:10.1016/j.polymdegradstab.2016.03.018

557 Bourmaud, A., Ausias, G., Lebrun, G., Tachon, M.-L.L., Baley, C., 2013. Observation of the
558 structure of a composite polypropylene/flax and damage mechanisms under stress. Ind.
559 Crops Prod. 43, 225–236. doi:10.1016/j.indcrop.2012.07.030

560 Bourmaud, A., Baley, C., 2007. Investigations on the recycling of hemp and sisal fibre
561 reinforced polypropylene composites. Polym. Degrad. Stab. 92, 1034–1045.
562 doi:10.1016/j.polymdegradstab.2007.02.018

563 Bourmaud, A., Beaugrand, J., Shah, D.., Placet, V., Baley, C., 2018. Towards the design of
564 high-performance plant fibre composites. Prog. Mater. Sci. 97, 347–408.

565 Bourmaud, A., Corre, Y.-M., Baley, C., 2015. Fully biodegradable composites: Use of poly-
566 (butylene-succinate) as a matrix and to plasticize l-poly-(lactide)-flax blends. Ind. Crops
567 Prod. 64, 251–257. doi:10.1016/j.indcrop.2014.09.033

568 Bourmaud, A., Le Duigou, A., Gourier, C., Baley, C., 2016b. Influence of processing
569 temperature on mechanical performance of unidirectional polyamide 11-flax fibre
570 composites. Ind. Crops Prod. 84, 151–165. doi:10.1016/j.indcrop.2016.02.007

571 Bourmaud, A., Morvan, C., Baley, C., 2010. Importance of fiber preparation to optimize the
572 surface and mechanical properties of unitary flax fiber. Ind. Crops Prod. 32, 662–667.
573 doi:http://dx.doi.org/10.1016/j.indcrop.2010.08.002

574 Di Giuseppe, E., Castellani, R., Dobosz, S., Malvestio, J., Berzin, F., Beaugrand, J., Delisée,
575 C., Vergnes, B., Budtova, T., 2016. Reliability evaluation of automated analysis, 2D
576 scanner, and micro-tomography methods for measuring fiber dimensions in polymer-
577 lignocellulosic fiber composites. Compos. Part A Appl. Sci. Manuf. 90, 320–329.
578 doi:10.1016/j.compositesa.2016.07.020

579 Duigou, A. Le, Castro, M., 2017. Hygromorph BioComposites: Effect of fibre content and
580 interfacial strength on the actuation performances. Ind. Crops Prod. 99, 142–149.
581 doi:https://doi.org/10.1016/j.indcrop.2017.02.004

582 Felix, J.M., Gatenholm, P., 1991. The nature of adhesion in composites of modified cellulose
583 fibers and polypropylene. J. Appl. Polym. Sci. 42, 609–620.
584 doi:10.1002/app.1991.070420307

585 Ferreira, P.J., Matos, S., Figueiredo, M.M., 1999. Size Characterization of Fibres and Fines in
586 Hardwood Kraft Pulps. Part. Part. Syst. Charact. 16, 20–24. doi:10.1002/(SICI)1521-
587 4117(199905)16

588 Gallos, A., Paes, G., Legland, D., Allais, F., Beaugrand, J., 2017. Exploring the microstructure
589 of natural fibre composites by confocal Raman imaging and image analysis. Compos.
590 Part A Appl. Acience Manuf. 94, 32–40.

591 Goudenhooft, C., Bourmaud, A., Baley, C., 2019. Study of plant gravitropic response:
592 Exploring the influence of lodging and recovery on the mechanical performances of flax
593 fibers. Ind. Crops Prod. 128, 235–238. doi:https://doi.org/10.1016/j.indcrop.2018.11.024

594 Goudenhooft, C., Bourmaud, A., Baley, C., 2018. Conventional or greenhouse cultivation of
595 flax: What influence on the number and quality of flax fibers? Ind. Crops Prod. 123, 111–
596 117. doi:10.1016/j.indcrop.2018.06.066

597 Goudenhooft, C., Bourmaud, A., Baley, C., 2017. Varietal selection of flax over time: Evolution
598 of plant architecture related to influence on the mechanical properties of fibers. Ind. Crops
599 Prod. 97, 56–64. doi:10.1016/j.indcrop.2016.11.062

600 Gourier, C., Bourmaud, A., Le Duigou, A., Baley, C., 2017. Influence of PA11 and PP
601 thermoplastic polymers on recycling stability of unidirectional flax fibre reinforced
602 biocomposites. Polym. Degrad. Stab. 136, 1–9.
603 doi:10.1016/j.polymdegradstab.2016.12.003

604 Graupner, N., Rößler, J., Ziegmann, G., Müssig, J., 2014. Fibre/matrix adhesion of cellulose
605 fibres in PLA, PP and MAPP: A critical review of pull-out test, microbond test and single
606 fibre fragmentation test results. Compos. Part A Appl. Sci. Manuf. 63, 133–148.
607 doi:10.1016/j.compositesa.2014.04.011

608 Gupta, V., Mittal, R., Sharma, P., Mennig, G., Wolters, J., 1989. Some studies on glass fiber-
609 reinforced polypropylene. Part I: Reduction in fiber length during processing. Polym.
610 Compos. 10, 8–15.

611 Hughes, M., 2012. Defects in natural fibres: their origin, characteristics and implications for
612 natural fibre-reinforced composites. J. Mater. Sci. 47, 599–609. doi:10.1007/s10853-011-
613 6025-3

614 Khan, A.S., Man, Z., Bustam, M.A., Kait, C.F., Khan, M.I., Muhammad, N., Nasrullah, A., Ullah,
615 Z., Ahmad, P., 2016. Impact of Ball-Milling Pretreatment on Pyrolysis Behavior and
616 Kinetics of Crystalline Cellulose. Waste and Biomass Valorization 7, 571–581.
617 doi:10.1007/s12649-015-9460-6

618 Le Duc, A., Vergnes, B., Budtova, T., 2011. Polypropylene/natural fibres composites: Analysis
619 of fibre dimensions after compounding and observations of fibre rupture by rheo-optics.
620 Compos. Part A Appl. Sci. Manuf. 42, 1727–1737.
621 doi:http://dx.doi.org/10.1016/j.compositesa.2011.07.027

622 Le Duigou, A., Bourmaud, A., Balnois, E., Davies, P., Baley, C., 2012. Improving the interfacial
623 properties between flax fibres and PLLA by a water fibre treatment and drying cycle. Ind.
624 Crops Prod. 39, 31–39. doi:http://dx.doi.org/10.1016/j.indcrop.2012.02.001

625 Le Duigou, A., Bourmaud, A., Gourier, C., Baley, C., 2016. Multiscales shear properties of PA
626 11/ flax biocomposites. Compos. Part A Appl. Acience Manuf. 85, 123–129.
627 doi:10.1016/j.compositesa.2016.03.014

628 Le Moigne, N., Van den Oever, M., Budtova, T., 2011. A statistical analysis of fibre size and
629 shape distribution after compounding in composites reinforced by natural fibres. Compos.
630 Part A Appl. Acience Manuf. 42, 1542–1550.

631 Legland, D., Beaugrand, J., 2013. Automated clustering of lignocellulosic fibres based on
632 morphometric features and using clustering of variables. Ind. Crops Prod. 45, 253–261.
633 doi:10.1016/j.indcrop.2012.12.021

634 Mohanty, A.K., Vivekanandhan, S., Pin, J.-M., Misra, M., 2018. Composites from renewable
635 and sustainable resources: Challenges and innovations. Science (80-.). 362, 536–542.
636 doi:10.1126/science.aat9072

637 Nada, S., Ivan, Š., Mirko, S., Antun, T., András, J., Josef, S., Peter, Z., 1998. An X-Ray
638 Diffraction Study of the Crystalline to Amorphous Phase Change in Cellulose During High-
639 Energy Dry Ball Milling. Holzforsch. - Int. J. Biol. Chem. Phys. Technol. Wood 52, 455–
640 458. doi:10.1515/hfsg.1998.52.5.455

641 Rabinowitsch, B., 1929. Über die Viskosität und Elastizität von Solen. Physik.Chemie 145A,
642 1–26.

643 Renouard, N., Mérotte, J., Kervoëlen, A., Behlouli, K., Baley, C., Bourmaud, A., 2017.
644 Exploring two innovative recycling ways for poly-(propylene)-flax non wovens wastes.
645 Polym. Degrad. Stab. 142, 89–101. doi:10.1016/j.polymdegradstab.2017.05.031

646 Schell, D.J., Harwood, C., 1994. Milling of lignocellulosic biomass. Appl. Biochem. Biotechnol.
647 45, 159–168. doi:10.1007/BF02941795

648 Steller, R.T., 2005. Rheological behavior of polymer melts with natural fibers. J. Appl. Polym.
649 Sci. 97, 1401–1409. doi:10.1002/app.21156

650 Tanguy, M., Bourmaud, A., Beaugrand, J., Gaudry, T., Baley, C., 2018. Polypropylene
651 reinforcement with flax or jute fibre; Influence of microstructure and constituents
652 properties on the performance of composite. Compos. Part B Eng. 139, 64–74.
653 doi:10.1016/j.compositesb.2017.11.061

654 Tarafdar, J.C., Meena, S.C., Kathju, S., 2001. Influence of straw size on activity and biomass

655 of soil microorganisms during decomposition. Eur. J. Soil Biol. 37, 157–160.
656 doi:https://doi.org/10.1016/S1164-5563(01)01084-6

657 Teuber, L., Militz, H., Krause, A., 2016. Dynamic particle analysis for the evaluation of particle
658 degradation during compounding of wood plastic composites. Compos. Part A Appl. Sci.
659 Manuf. 84, 464–471. doi:https://doi.org/10.1016/j.compositesa.2016.02.028

660 Thygesen, L.G., Thybring, E.E., Johansen, K.S., Felby, C., 2014. The Mechanisms of Plant
661 Cell Wall Deconstruction during Enzymatic Hydrolysis. PLoS One 9, 1–4.
662 doi:10.1371/journal.pone.0108313

663

664

Table caption

Table 1. Mechanical properties of elementary flax fibers (Bourmaud et al., 2015).

Table 2. Formulations of the different composites. ‘F’ represents fibres and ‘f’ represents fines.

Table 3. Morphometric characteristics of the reinforcement after injection.

Figure captions

Figure 1. Screw profiles and fibres/fines/chalk introduction area on the twin-screw extrusion system.

Figure 2. SEM images of flax fibres (A), flax fines (B) and chalk (C).

Figure 3. Distribution of fibre and particle size before incorporation into the composites.

Figure 4. Thermal degradation of flax fibres and fines

Figure 5. Young’s modulus (A) and strength at break (B) of flax fines and fibres PP/PPgMA composites for a range of reinforcement volume fractions.

Figure 6. Influence of the reinforcement on the rheological properties of the composite. Example of PP composites.

Figure 7. Tensile Young’s modulus (A) and strength at max (B) of the different composites

Figure 8. Impact energy of the different composites. No breakage with this test occurred for pure polymers, therefore results are not shown.

Figure 1. Screw profiles and fibres/fines/chalk introduction areas on the twin-screw extrusion system.

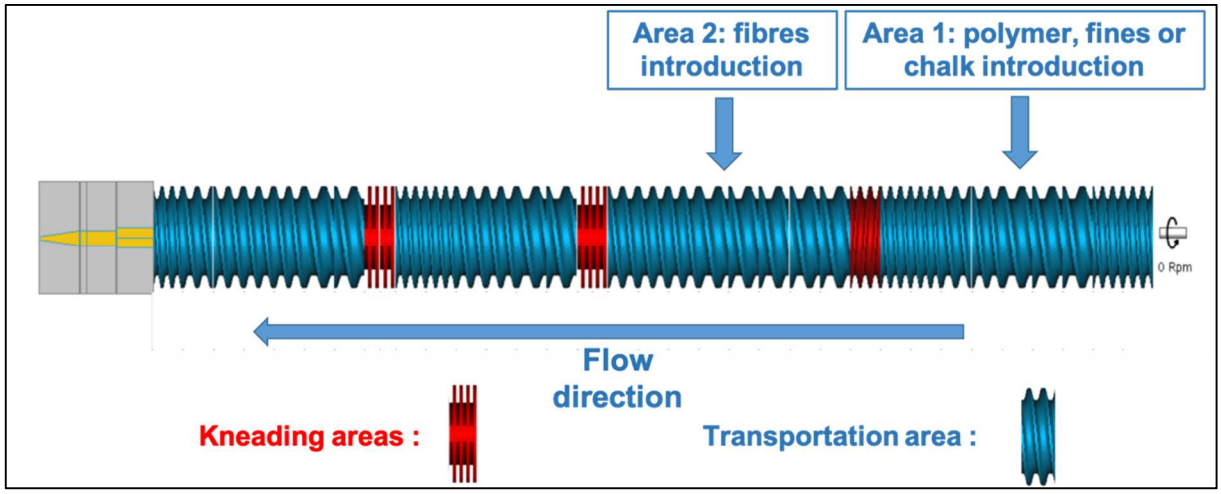

Figure 2. SEM images of flax fibres (A), flax fines (B) and chalk (C)

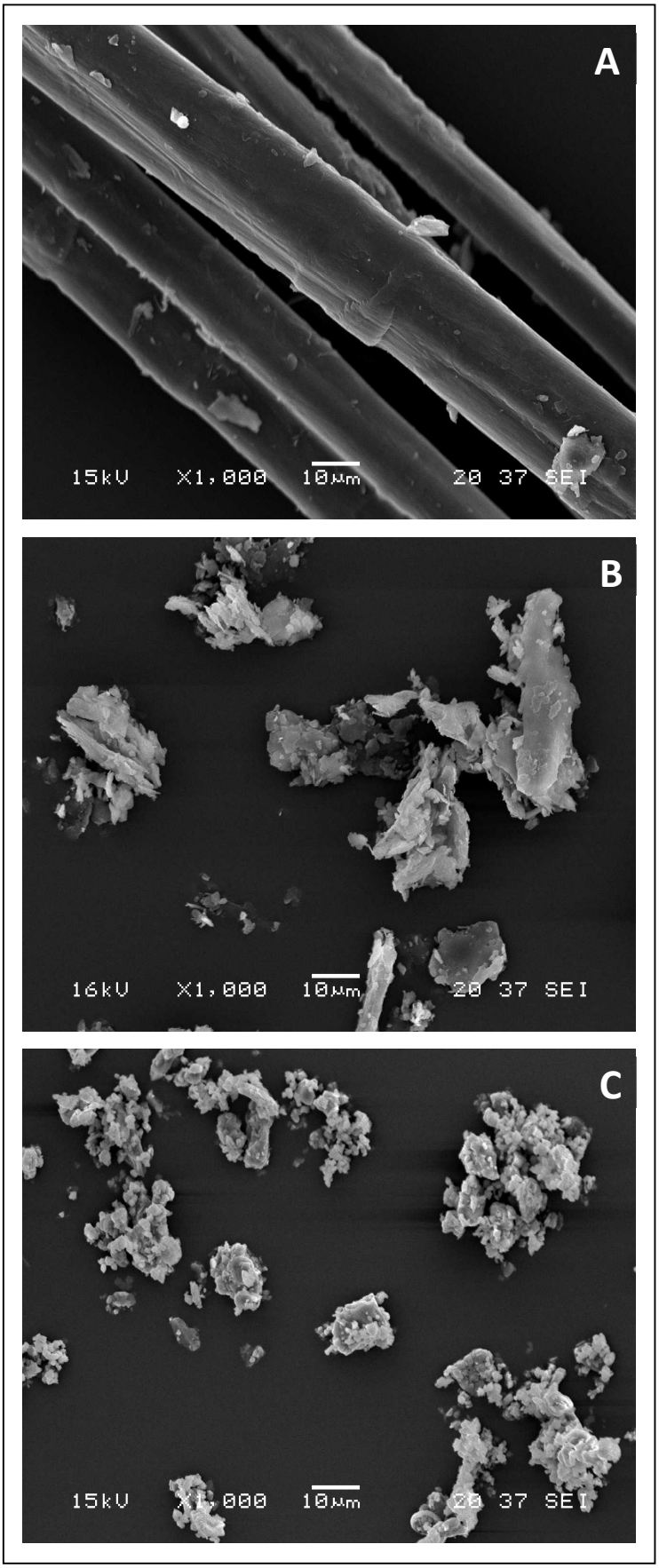

Figure 3. Distribution of fibre and particle size before incorporation into the composites.

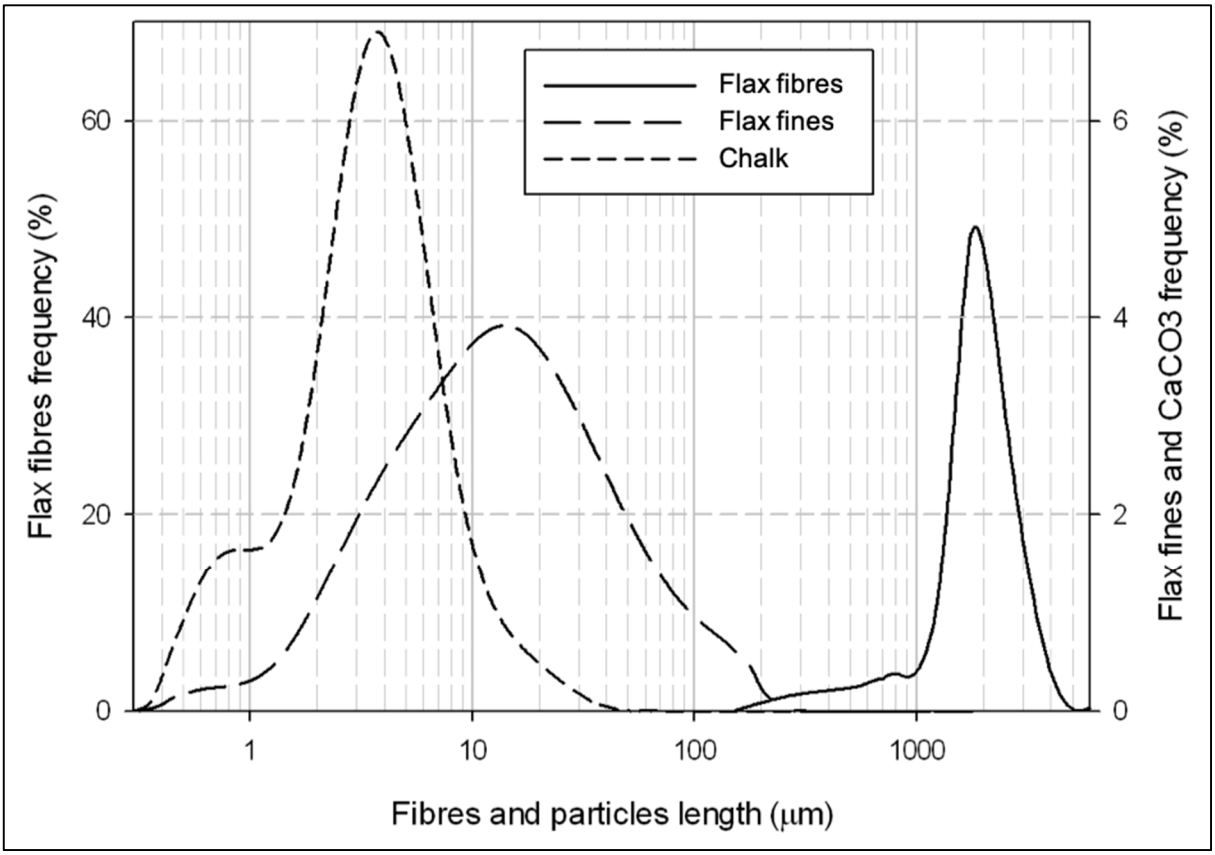

Figure 4. Thermal degradation of flax fibre and fines

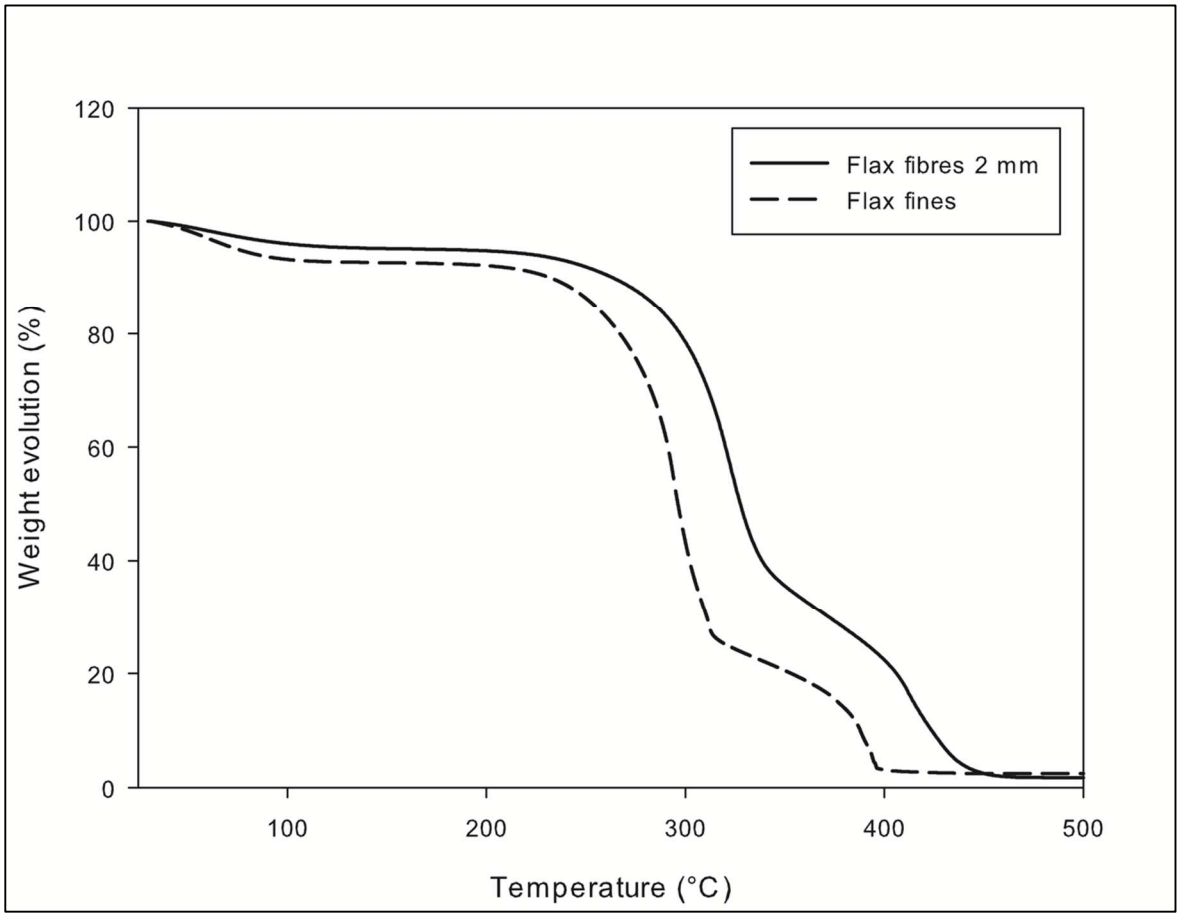

Figure 5. Young's modulus (A) and strength at break (B) of flax fines and fibres PP/PPgMA composites for a range of reinforcement volume fractions.

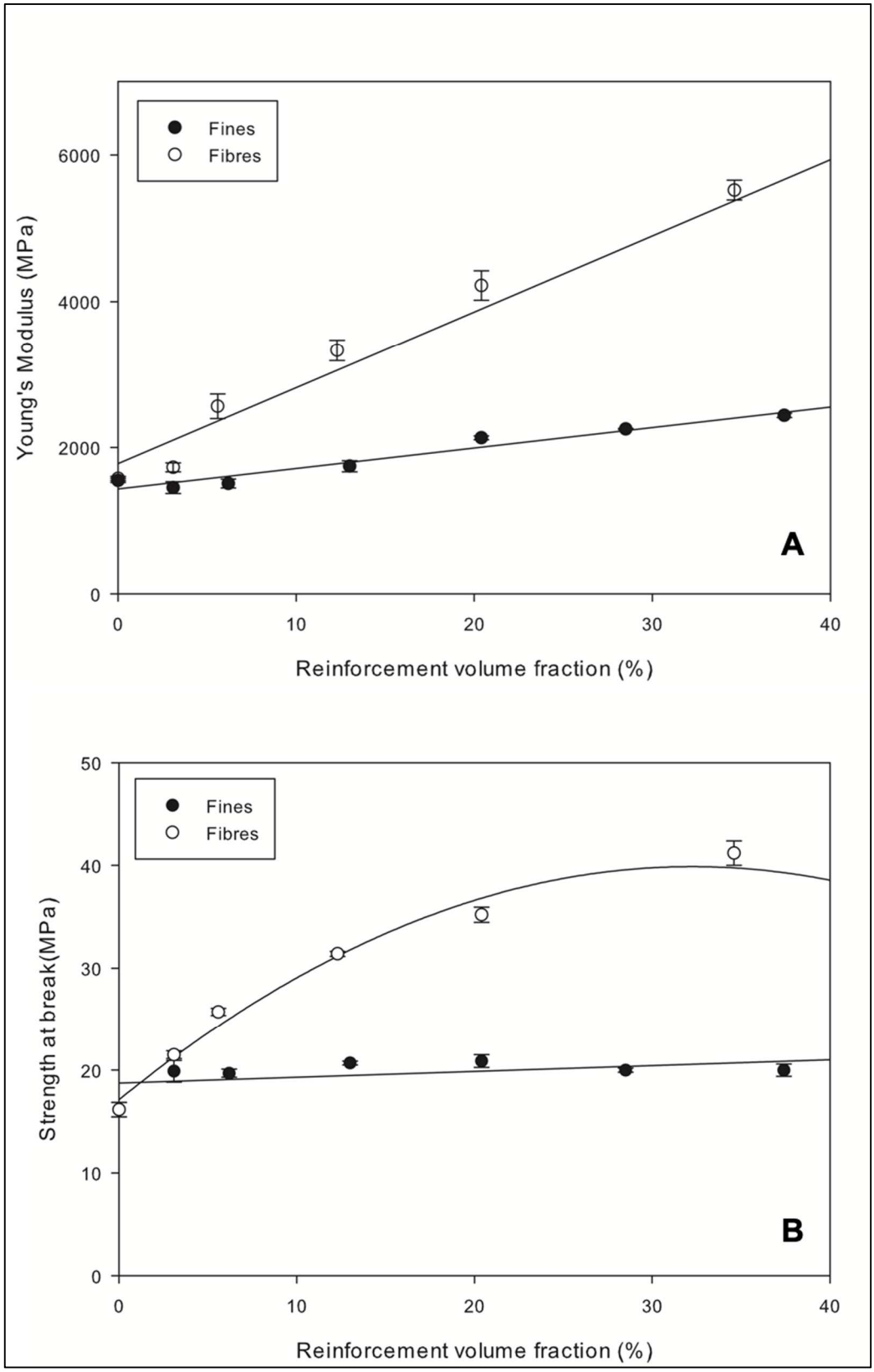

Figure 6. Influence of the reinforcement on the rheological properties of the composite. Example of PP composites.

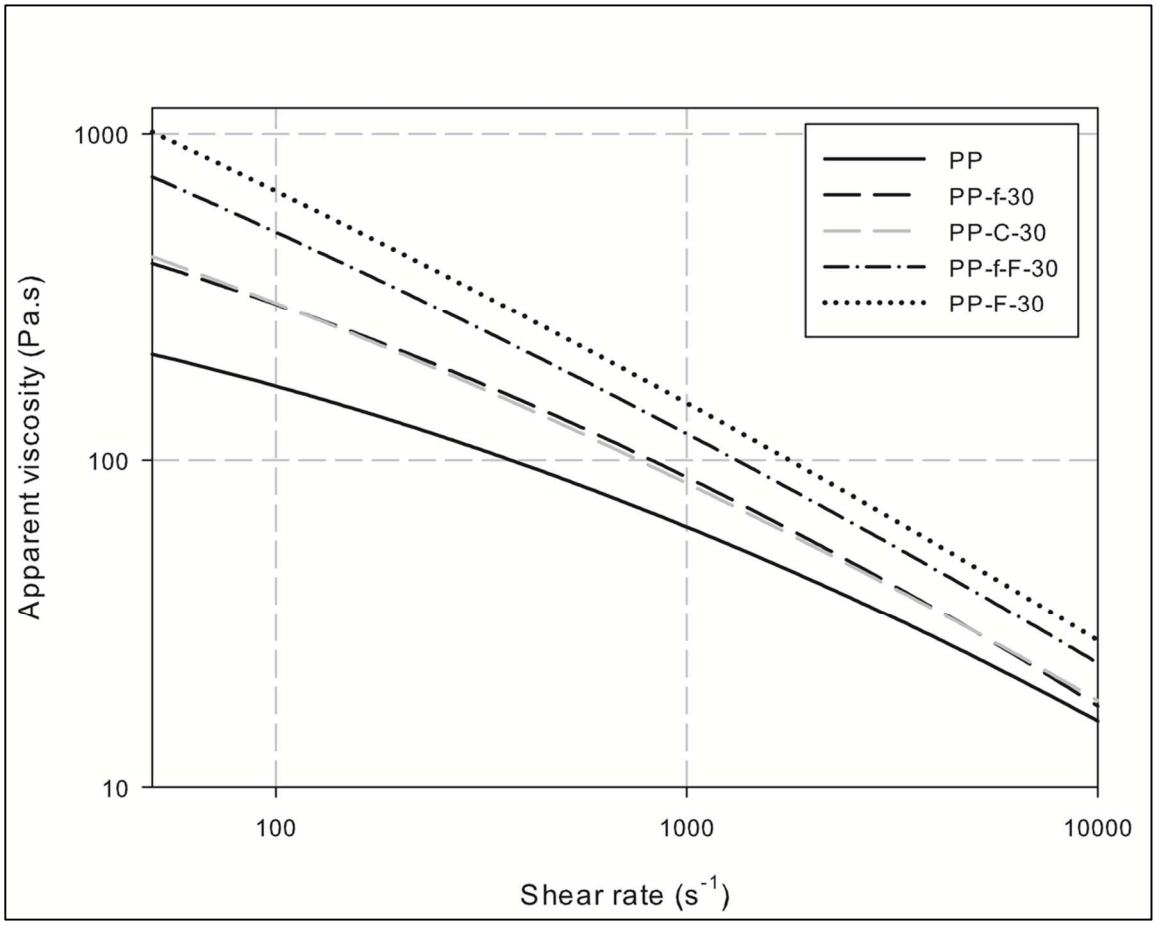

Figure 7. Tensile Young's modulus (A) and strength at max (B) of the different composites

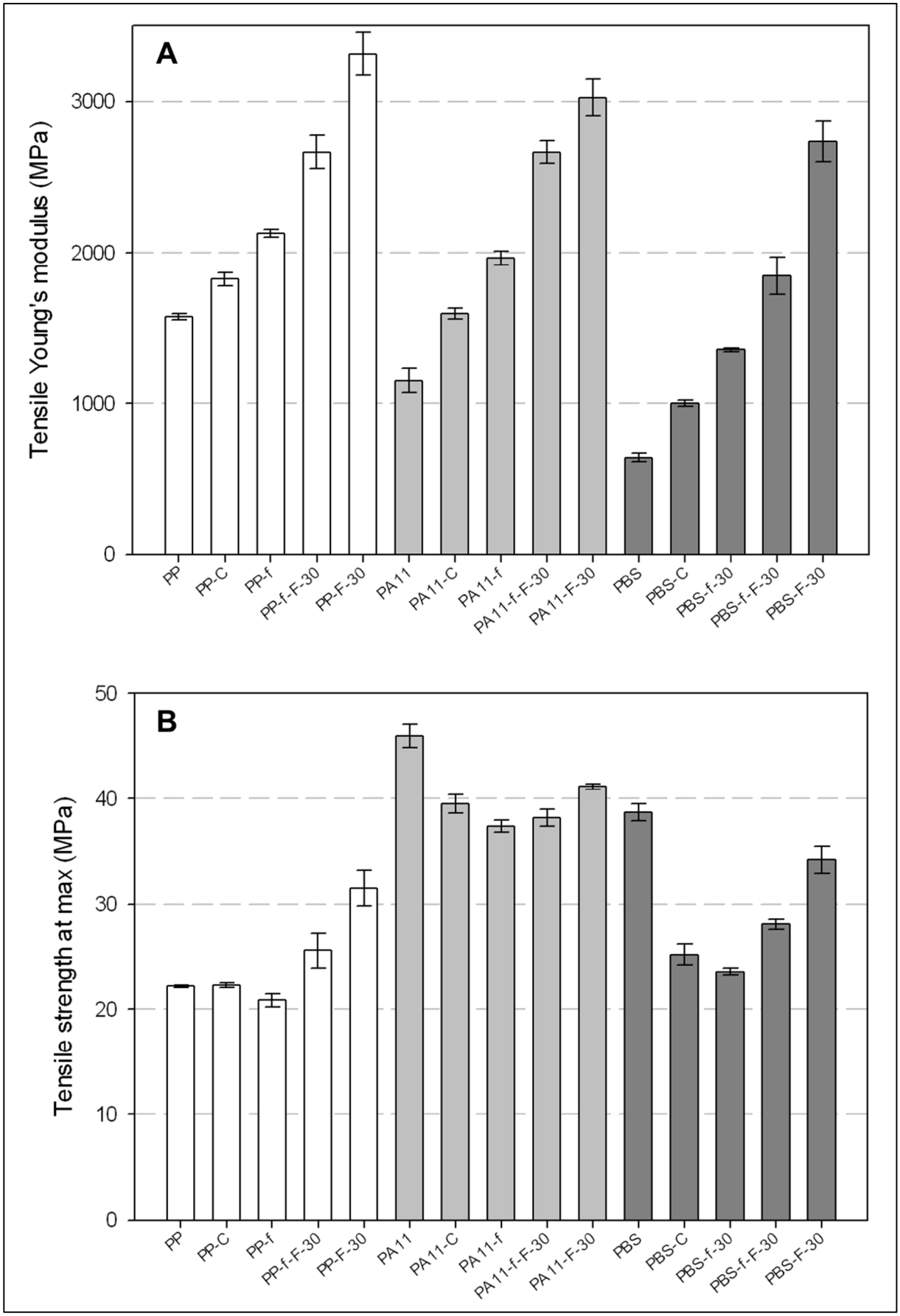

Figure 8. Impact energy of the different composites. No breakage with this test occurred for pure polymers, therefore results are not shown.

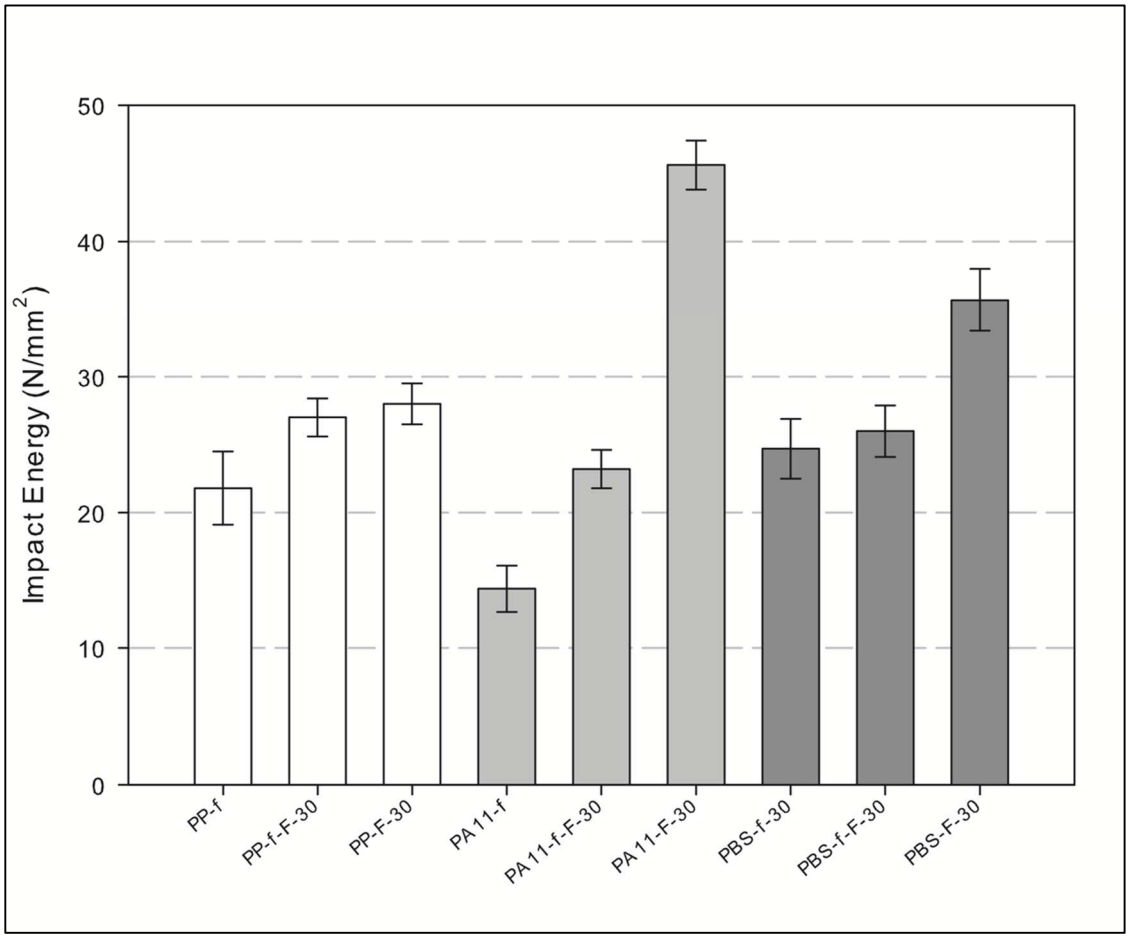

Table 1. Mechanical properties of elementary flax fibers (Bourmaud et al., 2015).

Materials	Number of fibers	Diameter (µm)	Young's modulus (GPa)	Strength at break (MPa)	Elongation at break (%)
Marylin flax fibers	90	15.5 ± 2.7	53.8 ± 14.3	1215 ± 500	2.24 ± 0.59

Table 2. Formulations of the different composites, 'F' represents fibres and 'f' represents fines.

Sample	PP/PP-g-MA mass fraction (%)	PBS mass fraction (%)	PA11 mass fraction (%)	Fibres mass (and volume) fraction (%)	Fines mass (and volume) fraction (%)	Chalk mass (and volume) fraction (%)
PP-PPgMA	100	0	0	0	0	0
PBS	0	100	0	0	0	0
PA11	0	0	100	0	0	0
PP-f-5	95	0	0	0	5 (3.1)	0
PP-f-10	90	0	0	0	10 (6.2)	0
PP-f-20	80	0	0	0	20 (13.0)	0
PP-f-30	70	0	0	0	30 (20.4)	0
PP-f-40	60	0	0	0	40 (28.5)	0
PP-f-50	50	0	0	0	50 (37.4)	0
PP-F-5	95	0	0	5 (3.1)	0	0
PP-F-9	90	0	0	9 (5.6)	0	0
PP-F-19	80	0	0	19 (12.3)	0	0
PP-F-30	70	0	0	30 (20.4)	0	0
PP-F-47	60	0	0	47 (34.6)	0	0
PP-F-53	50	0	0	53 (40.2)	0	0
PP-f-F-30	70	0	0	15 (9.5)	15 (9.5)	0
PP-C-30	70	0	0	0	0	30 (12.7)
PBS-f-30	0	70	0	0	30 (20.4)	0
PBS-f-F-30	0	70	0	15 (9.5)	15 (9.5)	0
PBS-F-30	0	70	0	30 (20.4)	0	0
PBS-C-30	0	70	0	0	0	30 (12.7)
PA11-f-30	0	0	70	0	30 (20.4)	0
PA11-f-F-30	0	0	70	15 (9.5)	15 (9.5)	0
PA11-F-30	0	0	70	30 (20.4)	0	0
PA11-C-30	0	0	70	0	0	30 (12.7)

Table 3. Morphometric characteristics of the reinforcement after injection.

Sample	Lw (µm)	Dw (µm)	L/D (-)
PP-f-30	225±6	42±2	5±0.2
PP-f-F-30	430±100	39±8	11±2.0
PP-F-30	592±183	18±6	31±4.0
PA11-F-30	434±35	36±9	12±3.0
PBS-F-30	497±19	14±1	38±0.5